

Rapid Communications

The Rapid Communications section is intended for the accelerated publication of important new results. Since manuscripts submitted to this section are given priority treatment both in the editorial office and in production, authors should explain in their submittal letter why the work justifies this special handling. A Rapid Communication should be no longer than 3½ printed pages and must be accompanied by an abstract. Page proofs are sent to authors, but, because of the accelerated schedule, publication is not delayed for receipt of corrections unless requested by the author or noted by the editor.

Search for single photons from radiative neutrino or supersymmetric-particle production

W. T. Ford, N. Qi, A. L. Read, Jr., and J. G. Smith

Department of Physics, University of Colorado, Boulder, Colorado 80309

T. Camporesi, I. Peruzzi, and M. Piccolo

Istituto Nazionale di Fisica Nucleare, Laboratori Nazionali di Frascati, Frascati, Italy

R. B. Hurst, K. H. Lau, J. Pyrlík, J. P. Venuti, H. B. Wald, and R. Weinstein

Department of Physics, University of Houston, Houston, Texas 77004

H. R. Band, M. W. Gettner, G. P. Goderre, J. H. Moromisato, W. D. Shambroom,* J. C. Sleeman, and E. von Goeler

Department of Physics, Northeastern University, Boston, Massachusetts 02115

W. W. Ash, G. B. Chadwick, R. E. Leedy, R. L. Messner, L. J. Moss, F. Muller,† H. N. Nelson, D. M. Ritson,
L. J. Rosenberg, D. E. Wiser, and R. W. Zdarko

Department of Physics and Stanford Linear Accelerator Center, Stanford University, Stanford, California 94305

D. E. Groom and P. G. Verdini

Department of Physics, University of Utah, Salt Lake City, Utah 84112

M. C. Delfino, J. R. Johnson, T. L. Lavine, T. Maruyama, and R. Prepost

Department of Physics, University of Wisconsin, Madison, Wisconsin 53706

(Received 20 March 1986)

A search for single photons produced in association with neutrinos or other weakly interacting neutral particles has been performed in e^+e^- annihilations at $\sqrt{s} = 29$ GeV with the MAC detector at the SLAC e^+e^- storage ring PEP. One event is observed, with 1.1 events expected from the reaction $e^+e^- \rightarrow \nu\bar{\nu}\gamma$. The number of neutrino families is restricted to $N_\nu < 17$ at the 90% confidence level. Limits on possible masses of supersymmetric electrons (\tilde{e}) and photons ($\tilde{\gamma}$) are presented. The \tilde{e} mass limit is $m_{\tilde{e}} > 48$ GeV/ c^2 at the 90% confidence level if $m_{\tilde{e}_L} = m_{\tilde{e}_R}$ and $m_{\tilde{\gamma}} = 0$. If $m_{\tilde{e}_L} \gg m_{\tilde{e}_R}$, the corresponding limit is $m_{\tilde{e}_R} > 40$ GeV/ c^2 .

Searches for photons from the reaction $e^+e^- \rightarrow \tilde{\gamma}\tilde{\gamma}\gamma$ currently provide the most restrictive limits on the masses of possible supersymmetric partners to the electron (\tilde{e}) and photon ($\tilde{\gamma}$) in models where the $\tilde{\gamma}$ is light and stable.^{1,2} A dominant background to these searches, the reaction $e^+e^- \rightarrow \nu\bar{\nu}\gamma$, is also of considerable interest since the cross section integrated over all angles is proportional to $(1 + N_\nu/4)$ (Ref. 3), where N_ν is the number of light-neutrino families. Present limits on N_ν from e^+e^- , although not quite as restrictive as recent $\bar{p}p$ collider results,⁴ provide an independent measurement of this fundamental quantity. This paper reports a search for single photons accompanied by weakly interacting particles in three data samples totaling 177 pb⁻¹ of e^+e^- interactions accumulated by the MAC detector on the PEP storage ring at SLAC. Improved selection criteria, complete use of all small-angle detectors, and an additional

61 pb⁻¹ of integrated luminosity have allowed significant improvement in the limits on radiative neutrino and supersymmetric-particle production compared with our previously published search.¹

Although supersymmetric (SUSY) theories⁵ continue to generate much theoretical activity, none of the predicted partners to ordinary particles has yet been found. In many SUSY models the lightest SUSY particle is neutral, stable, interacts only weakly with matter, and thus cannot be directly detected. Two candidates for this lightest SUSY particle which can be produced in e^+e^- interactions are the $\tilde{\gamma}$ produced via virtual \tilde{e} exchange and the scalar neutrino ($\tilde{\nu}$) produced via Z or supersymmetric- W (\tilde{W}) exchange. The cross section for radiative production of $\tilde{\gamma}$ or $\tilde{\nu}$ pairs is a function of both the $\tilde{\gamma}$ or $\tilde{\nu}$ masses and the masses of the exchanged particles.⁶ These cross sections are comparable

to the radiative neutrino process if $m_{\tilde{\nu}} = 0$ and $m_{\tilde{e}} = 52$ GeV/ c^2 or if $m_{\tilde{\nu}} = 13$ GeV/ c^2 and $m_{\tilde{W}} = 29$ GeV/ c^2 .

Photons from $e^+e^- \rightarrow \nu\bar{\nu}\gamma$, $\tilde{\gamma}\tilde{\gamma}\gamma$, and $\tilde{\nu}\tilde{\nu}\gamma$ have similar energy and angular distributions, peaked sharply at low energy and at small polar angles. Other radiative processes, $e^+e^- \rightarrow e^+e^-\gamma$, $\gamma\gamma\gamma$, $\mu^+\mu^-\gamma$, and $\tau^+\tau^-\gamma$ can also produce single-photon events if the other particles in the event are lost into uninstrumented or inefficient regions of the detector. For a detector completely efficient above some polar angle relative to the beam axis, the background from $e^+e^-\gamma$, $\gamma\gamma\gamma$, and $\mu^+\mu^-\gamma$ is kinematically limited to

$$E_{1\gamma} \leq (\sqrt{s} - E_{\gamma}) \sin\theta_{\text{veto}} .$$

$E_{1\gamma}$ is the transverse energy of the detected photon and θ_{veto} is the maximum polar angle of undetected particles. This restriction does not apply to $e^+e^- \rightarrow \tau^+\tau^-\gamma$ where decay neutrinos may carry significant momentum. However, given the photon energy resolution, the luminosity, and θ_{veto} , the background from all of these processes is easily calculated. The data in this report were collected in three running periods of differing θ_{veto} . The single-photon search region for each period was chosen accordingly.

The MAC detector, composed of calorimetric and tracking chambers covering $> 98\%$ of 4π sr, has been described in previous reports.⁷ Of particular importance to this experiment are the electromagnetic shower calorimeter (SC) in which photon energies and directions are measured, and the end-cap calorimeters (EC's) and small-angle detectors which define θ_{veto} . The other MAC detector elements (inner and outer drift chambers, hadron calorimeters, and scintillation counters) provide rejection of cosmic-ray, single-electron, and beam-gas backgrounds. The 14-radiation-length (r.l.) SC, constructed from alternating planes of lead and proportional wire chambers (PWC's) covering $35^\circ < \theta < 145^\circ$, is segmented radially into three layers. Position information is derived from 1.9° azimuthal segments digitized at both ends. The angular resolution has been determined from radiative Bhabha scattering events to be 1.3° in azimuth (ϕ) and 1.7° in the polar angle (θ). The energy resolution is $\sigma_E/E = 20\%/\sqrt{E}$ (GeV).

The first data sample of 36 pb^{-1} was collected with the original detector configuration. End-cap calorimeters covered polar angles greater than 10° with at least 20 r.l. of steel and PWC planes. A single plane of scintillators provided redundant coverage to about 12° from the beam axis. Fully efficient small-angle veto calorimeters (SAV's) covering $3.8^\circ < \theta < 17.5^\circ$ were installed for the second data sample of 80 pb^{-1} . Downstream of the SAV detectors, small-angle tagging counters (SAT's) cover 85% of the azimuth between $2.5^\circ < \theta < 6.2^\circ$. Each SAV was constructed from alternating discs of lead and PWC planes totaling 8.5 r.l. Each SAT was made from 6–8 r.l. of lead backed by 2 cm of plastic scintillators. Mechanical supports for the beam pipe precluded complete azimuthal coverage for the SAT's. A vertex chamber (VC) was installed for the last data sample of 61 pb^{-1} . The additional shielding necessary for the VC obstructed the SAV's and SAT's below 6.8° . Rings of 24 bismuth germanate (BGO) crystals with photodiode readout were added between the VC and shielding, recovering part of the lost veto coverage. These BGO rings cover $4.8^\circ < \theta < 7.2^\circ$ with 10 r.l. of active material.

Data for this experiment were collected with a single-photon trigger requiring energy deposition in at least two of the

SC layers and a minimum of 1 GeV of energy in good time coincidence (± 75 nsec) with the beam crossing. Subsequent data analysis required that candidate events have a photon well inside the SC, $40^\circ < \theta_\gamma < 140^\circ$, and that no evidence of other particles appear in any of the other parts of the detector. Cuts applied on the energy-deposition pattern were designed to eliminate photons not originating from the beam-interaction vertex. A detailed description of the event selection follows.

Photon showers were recognized by a clustering algorithm that combined calorimeter hits above 100 MeV from the SC, EC, and hadron calorimeters with neighboring hits in ϕ and θ . The minimum cluster contains two hits. Clusters were allowed to extend into the hadron calorimeter. Each shower was assigned energy E and angles θ and ϕ from the scalar and vector sum of its individual hits. Only events with a single cluster greater than 40° from the beam axis were kept. Single-electron events were eliminated by rejecting events with four or more central drift-chamber hits. Events with an outer drift-chamber track or with greater than 30% of the cluster energy in the hadron calorimeter were identified as cosmic rays and rejected.

The single-photon candidates surviving the above cuts were primarily $e^+e^-\gamma$ and $\gamma\gamma\gamma$ events, but contained small contributions from beam-gas and beam halo scatterings, and from noise in the SC. To further reduce these backgrounds, stringent cuts were made on the shower profile. Every shower was required to have one or more hits in the first layer of the SC and two or more hits in the second layer. For this analysis it was further required that the shower have at least one hit in the third layer of the SC. These cuts have a strong bias against photons from beam related backgrounds entering the SC at shallow angles. Cuts on the angular width in ϕ and θ of candidate showers further rejected events not originating at the beam vertex. The hits in each shower were fit to a straight line not constrained to the event vertex. The point of intersection z_0 with the beam axis in the plane containing the beam axis and the shower centroid, and its distance of closest approach r_{min} to the interaction point in the plane transverse to the beam axis, were calculated with a resolution $\sigma_{z_0} = 12$ cm and $\sigma_{r_{\text{min}}} = 3.3$ cm. Showers were required to have $|z_0| < 30$ cm and $r_{\text{min}} < 15$ cm. Candidates passing these cuts were identified as single photons.

The selection criteria described were applied to all three running periods. Additional cuts on small-angle detectors installed after the first data period were made to reduce θ_{veto} . Events were vetoed if the energy in the SAV's was greater than 250 MeV. For the second data sample, events were also rejected if the SAT's were hit. The SAT's were not used in the third data sample. Instead, events with greater than 100 MeV in the BGO rings were rejected. The $E_{1\gamma}$ distributions of the single photons satisfying these requirements are shown in Fig. 1 for the three data samples.

Trigger, detection, and analysis efficiencies were determined as a function of $E_{1\gamma}$ and θ_γ from radiative Bhabha scattering events with a single electron or photon in the SC and at least 3 GeV deposited in the SAV's. Losses due to background noise in the SAV, SAT, BGO, drift, calorimeter, and scintillator detectors were studied with beam crossings selected at random. The photon conversion probability in the beam pipe was determined from Monte Carlo studies⁸

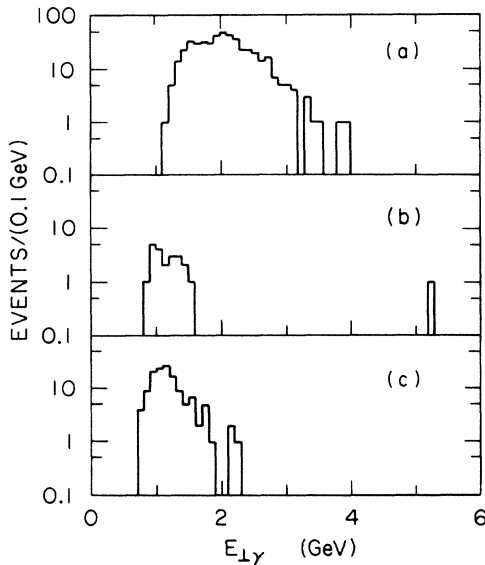


FIG. 1. (a) $E_{\perp\gamma}$ spectrum of single photons for the first data sample of 36 pb^{-1} with $\theta_{\text{veto}} = 10^\circ$ and search region $E_{\perp\gamma} > 4.5 \text{ GeV}/c^2$. (b) $E_{\perp\gamma}$ spectrum for the second data sample of 80 pb^{-1} with $\theta_{\text{veto}} = 2.5^\circ$ and search region $E_{\perp\gamma} > 2.0 \text{ GeV}/c^2$. (c) $E_{\perp\gamma}$ spectrum for the third data sample of 61 pb^{-1} with $\theta_{\text{veto}} = 4.5^\circ$ and search region $E_{\perp\gamma} > 2.6 \text{ GeV}/c^2$.

to be 2–5% depending on the running period. An overall efficiency for each data sample was calculated from the product of the above efficiencies as a function of $E_{\perp\gamma}$ and θ_γ . This efficiency typically rises from 53% at $E_{\perp\gamma} = 2.0 \text{ GeV}$ to 69% at $E_{\perp\gamma} = 4.5 \text{ GeV}$.

The expected yield of single photons from $e^+e^- \gamma$, $\gamma\gamma\gamma$, $\mu^+\mu^-\gamma$, and $\tau^+\tau^-\gamma$ events passing the trigger and analysis cuts was compared to the data for each of the running periods. A Monte Carlo generator⁹ produced events which were then smeared with the MAC energy and angular resolution functions. The $E_{\perp\gamma}$ spectrum of photons in the geometric acceptance corrected for the detector efficiency was determined for each different θ_{veto} . The best θ_{veto} fit to each data sample agreed with the angles expected from the geometry of the small angle detectors. A separate analysis of single-electron events from $e^+e^- \gamma$ verified the θ_{veto} determined by this procedure.

A search region for each of the running periods was defined such that the combined background from $e^+e^- \gamma$, $\gamma\gamma\gamma$, $\mu^+\mu^-\gamma$, and $\tau^+\tau^-\gamma$ events was expected to be less than 0.1 event for each data period. The search regions are (a) $E_{\perp\gamma} > 4.5 \text{ GeV}$, (b) $E_{\perp\gamma} > 2.0 \text{ GeV}$, and (c) $E_{\perp\gamma} > 2.6 \text{ GeV}$. The expected yield of photons from $e^+e^- \rightarrow \nu\bar{\nu}\gamma$ ($N_\nu = 3$) was 0.1 in (a), 0.6 in (b), and 0.4 in (c). Only the previously reported event at $E_{\perp\gamma} = 5.3 \text{ GeV}$ is found in the search regions. The yield of photons from $e^+e^- \gamma$, $\gamma\gamma\gamma$, and $\mu^+\mu^-\gamma$ events falls steeply with $E_{\perp\gamma}$ and cannot account for the observed event. Calculations of the $E_{\perp\gamma}$ spectra of photons from $\tau^+\tau^-\gamma$ show a much flatter $E_{\perp\gamma}$ dependence and predict a total of 0.03 events for $E_{\perp\gamma} > 4.5 \text{ GeV}$. The most likely hypothesis is that the observed event is from $\nu\bar{\nu}\gamma$ production since 45% of the expected 1.1 neutrino events have $E_{\perp\gamma} > 4.5 \text{ GeV}$. Observing one event in the three search regions corresponds to a limit of $N_\nu < 17$ at the 90% confidence level with no SUSY or background produc-

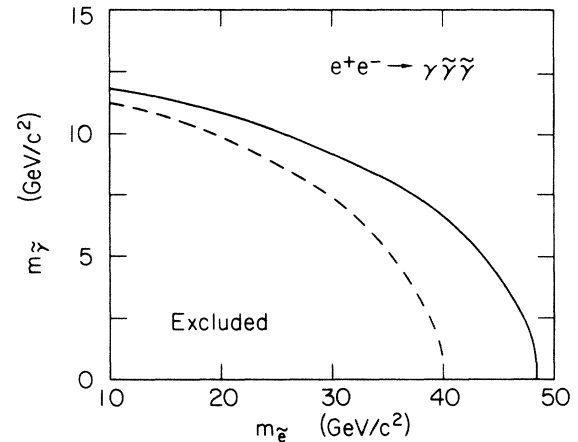


FIG. 2. The lower limit for $m_{\tilde{e}}$ as a function of $m_{\tilde{\gamma}}$. The solid curve is for $m_{\tilde{e}_L} = m_{\tilde{e}_R}$. The dashed curve is for $m_{\tilde{e}_L} \gg m_{\tilde{e}_R}$. The limits are at the 90% confidence level.

tion assumed or subtracted. The cross-section upper limit equivalent to this neutrino-family limit is 26.5 fb at the 90% confidence level for $E_{\perp\gamma} > 3.0 \text{ GeV}$ and $40^\circ < \theta_\gamma < 140^\circ$.

Since the search regions have different $E_{\perp\gamma}$ thresholds and the efficiency varies with $E_{\perp\gamma}$, a differential cross section must be specified before a cross-section limit can be calculated from the combined data. Limits on anomalous single-photon production were calculated after subtracting the expected $\nu\bar{\nu}\gamma$ background. The upper limit on anomalous single-photon production is 18.8 fb at the 90% confidence level for $E_{\perp\gamma} > 3.0 \text{ GeV}$ and $40^\circ < \theta_\gamma < 140^\circ$ if the shape of the differential cross section is similar to $\nu\bar{\nu}\gamma$. Using the differential cross section for $\tilde{\gamma}\tilde{\gamma}\gamma$ production as calculated by Ware and Machacek,¹⁰ the regions of excluded \tilde{e} and $\tilde{\gamma}$ masses are shown in Fig. 2 for (a) $m_{\tilde{e}_L} = m_{\tilde{e}_R}$, and (b) $m_{\tilde{e}_L} \gg m_{\tilde{e}_R}$. For $m_{\tilde{\gamma}} = 0$ the limits are (a) $m_{\tilde{e}} > 48 \text{ GeV}/c^2$ and (b) $m_{\tilde{e}_R} > 40 \text{ GeV}/c^2$. These limits are significantly higher than those obtained from our previously published search¹ and greater than or comparable to results from other searches.²

The limits on $\tilde{\nu}$ and \tilde{W} masses depend on the specific SUSY model selected. A calculation by Grifols, Martínez, and Solà¹¹ of $\tilde{\nu}\tilde{\nu}\gamma$ production is used to obtain a limit for the $\tilde{\nu}$ mass of $m_{\tilde{\nu}} > 10.8 \text{ GeV}/c^2$ at the 90% confidence level if $m_{\tilde{W}} = 25 \text{ GeV}/c^2$. For $m_{\tilde{\nu}} = 0$ the limit is $m_{\tilde{W}} > 50 \text{ GeV}/c^2$ at the 90% confidence level.

We thank J. D. Ware and M. Martínez for providing the calculations of the $\tilde{\gamma}\tilde{\gamma}\gamma$ and $\tilde{\nu}\tilde{\nu}\gamma$ cross sections for the MAC detector acceptance. We also thank N. Erickson, J. Escalera, M. J. Frankowski, and J. Schroeder for technical assistance, and the SLAC staff for continued reliable operation of the PEP storage ring. We acknowledge the technical assistance and regret the passing of C. T. Pulliam. This work was supported in part by the U.S. Department of Energy under Contracts No. DE-AC02-81ER40025 (CU), No. DE-AC03-76SF00515 (SLAC), and No. DE-AC02-76ER00881 (UW); by the National Science Foundation under Contracts No. NSF-PHY82-15133 (UH), No. NSF-PHY82-15413, No. NSF-PHY82-15414 (NU), and No. NSF-PHY83-08135 (UU); and by the Istituto Nazionale di Fisica Nucleare.

*Also at Department of Physics and College of Computer Science, Northeastern University, Boston, MA 02215.

†Permanent address: CERN, Geneva, Switzerland.

¹MAC Collaboration, E. Fernandez *et al.*, Phys. Rev. Lett. **54**, 1118 (1985).

²JADE Collaboration, W. Bartel *et al.*, Phys. Lett. **152B**, 385 (1985); ASP Collaboration, G. Bartha *et al.*, Phys. Rev. Lett. **56**, 685 (1986).

³E. Ma and J. Okada, Phys. Rev. Lett. **41**, 287 (1978); **41**, 1759 (1978); K. J. F. Gaemers, R. Gastman, and F. M. Renard, Phys. Rev. D **19**, 1605 (1979).

⁴UA1 Collaboration, G. Arnison *et al.*, Phys. Lett. **166B**, 484 (1986).

⁵A recent and comprehensive review with references to the original literature is H. E. Haber and G. L. Kane, Phys. Rep. **117**, 75 (1985).

⁶J. A. Grifols, X. Mor-Mur, and J. Solà, Phys. Lett. **114B**, 35 (1982); P. Fayet, *ibid.* **117B**, 460 (1982); J. Ellis and J. S. Hagelin, *ibid.* **122B**, 303 (1983); J. S. Hagelin, G. L. Kane, and S. Raby, Nucl. Phys. **B241**, 638 (1984).

⁷W. T. Ford, in *Proceedings of the International Conference on Instrumentation for Colliding Beam Physics, Stanford, 1982*, edited by W. W. Ash (SLAC Report No. 250, 1982), p. 174.

⁸EGS, R. L. Ford and W. R. Nelson, SLAC Report No. SLAC-210, 1978.

⁹F. A. Berends, R. Kleiss, and S. Jadach, Nucl. Phys. **B202**, 63 (1982).

¹⁰J. Ware and M. E. Machacek, Phys. Lett. **142B**, 300 (1984); T. Kobayashi and M. Kuroda, *ibid.* **139B**, 208 (1984); K. Grassie and P. N. Pandita, Phys. Rev. D **30**, 22 (1984).

¹¹J. A. Grifols, M. Martínez, and J. Solà, Nucl. Phys. **B268**, 151 (1986).